Suspended sediment and discharge dynamics in a glacierized alpine environment: Identifying crucial areas and time periods on several spatial and temporal scales in the Ötztal, Austria

Lena Katharina Schmidt[1], Till Francke[1], Erwin Rottler[1], Theresa Blume[2], Johannes Schöber[3], Axel Bronstert[1]

[1]Institute of Environmental Sciences and Geography, University of Potsdam, Potsdam, 14476, Germany
[2]Section of Hydrology, GFZ German Research Centre for Geosciences, Potsdam, 14473, Germany
[3]Tiroler Wasserkraft AG (TiWAG), Innsbruck, 6020, Austria

Correspondence to: Lena Katharina Schmidt (leschmid@uni-potsdam.de)

Abstract. Climatic changes are expected to fundamentally alter discharge and sediment dynamics in glaciated high alpine areas, e.g. through glacier retreat, prolonged snow-free periods and more frequent intense rainfall events in summer. However, how exactly these hydrological changes will affect sediment dynamics is not yet known.

In the present study, we aim to pinpoint areas and processes most relevant to recent sediment and discharge dynamics on different spatial and temporal scales in the Ötztal Alpine Region in Tyrol, Austria. Therefore, we analyze observed discharge and relatively long suspended sediment time series of up to 15 years from three gauges in a nested catchment setup. The catchments range from 100 to almost 800 km² in size with 10 to 30 % glacier cover and span an elevation range of 930 to 3772 m a.s.l.. The investigation of satellite-based snow cover maps, glacier inventories, mass balances and precipitation data complement the analysis.

Our results indicate that mean annual specific discharge and suspended sediment fluxes are highest in the most glaciated sub-catchment and both fluxes correlate significantly with annual glacier mass balances. Furthermore, both discharge and suspended sediment loads show a distinct seasonality with low values during winter and high values during summer. However, the spring onset of sediment transport is almost synchronous at the three gauges, contrary to the spring rise in discharge, which occurs earlier further downstream.

A spatio-temporal analysis of snow cover evolution indicates that the spring increase in sediment fluxes at all gauges coincides with the onset of snow melt above 2500 m elevation. Zones above this elevation include glacier tongues and recently deglaciated areas, which seem to be crucial for the sediment dynamics in the catchment.

Precipitation events in summer were associated with peak sediment concentrations and fluxes, but on average accounted for only 21 % of the annual sediment yields of the years 2011 to 2020.

We conclude that glaciers and the areas above 2500 m elevation play a dominant role for discharge and sediment dynamics in the Ötztal area, while precipitation events play a secondary role. Our study extends the scientific knowledge on current hydro-sedimentological changes in glaciated high alpine areas and provides a baseline for investigations on projected future changes in hydro-sedimentological system dynamics.

1 Introduction

Glaciated high alpine areas are central for discharge and sediment dynamics even beyond their catchment boundaries because the discharge and sediment fluxes from these areas are typically much higher (per unit area) than from lower-lying areas (Beniston et al., 2018; Hallet et al., 1996; Hinderer et al., 2013; Milliman and Syvitski, 1992). As a consequence, glaciated high alpine areas have disproportionate influence on downstream water quality and quantity, flood hazard, hydropower generation and ecological habitats (Huss et al., 2017; Vercruysse et al., 2017).

Yet glaciated high alpine areas are also particularly sensitive to climatic change and climate warming is especially pronounced here (Gobiet et al., 2014). As a result of the rising temperatures, widespread and accelerating glacier retreat has been observed for several decades (e.g. Abermann et al., 2009; Sommer et al., 2020). Hydrological consequences include changes in water quantities (such as a transient increase in runoff) (Vormoor et al., 2015; Wijngaard et al., 2016), streamflow variability (Tiel et al., 2019) and hydrograph timing e.g. due to earlier snow-melt onset and a prolonged glacier melt period (Hanus et al., 2021; Kormann et al., 2016; Rottler et al., 2021, 2020).

Possible climate change impacts on sediment dynamics are manifold, as all of the hydrological changes can affect sediment dynamics by changing the magnitude and timing of transport capacities. At the same time, sediment supply may change as glacier retreat uncovers vast amounts of sediment previously inaccessible to pluvial and fluvial erosion (Carrivick and Heckmann, 2017; Leggat et al., 2015) and as subglacial sediment discharge transi-

55   ently increases (Delaney and Adhikari, 2020). Intense precipitation events, which are projected to increase in intensity and occur more frequently (Bürger et al., 2019; Giorgi et al., 2016; Scherrer et al., 2016), have a higher chance of affecting unfrozen material during prolonged snow-free periods (Kormann et al., 2016; Rottler et al., 2021; Wijngaard et al., 2016) and may thereby lead to a shift in the relative importance of sediment sources. Adding to this, permafrost thaw can destabilize hillslopes and facilitate mass movements (Chiarle et al., 2021;

60   Huggel et al., 2010; Savi et al., 2020). On the other hand, changes in catchment-scale connectivity can provide new pathways or close off old pathways for loose material to the receiving waters (Cavalli et al., 2013; Lane et al., 2017), for example due to the formation of a proglacial lake.

In order to inform mitigation and adaptation strategies, it is crucial to understand how changes in influencing factors and their complex interactions propagate to sediment dynamics, yet to date our understanding is still very

65   limited (Huss et al., 2017).

A first step towards facilitating the assessment of future changes is to understand discharge and sediment dynamics in the recent past and present. Studies that have embarked on this journey to date have either compared (mean) annual sediment yields across a number of sites (e.g. Delaney et al., 2018b; Hinderer et al., 2013; Lalk et al., 2014; Micheletti and Lane, 2016; Schöber and Hofer, 2018; Tschada and Hofer, 1990) or investigated dynamics in daily

70   or even finer temporal resolution but only at one or two locations (Beylich et al., 2017; Collins, 1996, 1990; Costa et al., 2018; Guillon et al., 2018; Leggat et al., 2015; Orwin and Smart, 2004; Swift et al., 2005; Tsyplenkov et al., 2020). However, it is crucial to consider discharge and sediment dynamics in high temporal resolution as well as their spatial patterns in rde to understand the dominant processes and thereby help inform modelling approaches that can put into perspective the effects of future changes.

75   In the present study, we aim to pinpoint the areas and processes most relevant to sediment dynamics in combination with discharge dynamics on several spatial and temporal scales. Our approach builds on three combined discharge and sediment gauges in a nested catchment setup in the Ötztal Alpine Region, where discharge data and relatively long suspended sediment time series of up to 15 years are available in high temporal resolution for catchments of 100 to almost 800 km² in size. To improve the existing sediment concentration data set, we improved the relation-

80   ship between turbidity and suspended sediment concentrations at the gauge in Sölden by operating an automatic water sampler. To complement our analysis, we investigate glacier inventories and mass balances, precipitation data, satellite-based snow cover maps and land cover characteristics.

More specifically, we (1) explore changes of magnitude and seasonality in discharge and suspended sediment fluxes across spatial scales, (2) analyze the seasonal distribution of both fluxes as well as the relative importance

85   of (precipitation) events for both fluxes as compared to snow and glacier melt and (3) examine the relative contributions of different elevation bands to sediment fluxes in spring using a synoptic view of snow cover evolution and sediment flux timing.

2 Methods

2.1. Study area

The study area is a nested catchment setup within the Ötztal valley in Tyrol, Austria (Fig. 1). The Ötztal Alps are part of the Ötztal-Stubai massif within the crystalline central Eastern Alps and biotite-plagioclase, biotite and muscovite gneisses, variable mica schists and gneissic schists dominate (Strasser et al., 2018). The entire catchment of 783 km² stretches from 931 m a.s.l. at the gauge in Tumpen (T) to 3772 m a.s.l. at the Wildspitze, the highest summit of Tyrol. Nested within are the 441 km² catchment of the gauge in Sölden (S) at 1343 m a.s.l. and the 98 km² catchment of the gauge in Vent (V) at 1891 m a.s.l. (Table 1). The areas in between the gauges Vent and Sölden (i.e. the area downstream of Vent and upstream of Sölden) and Sölden and Tumpen have been termed S-V and T-S, respectively.
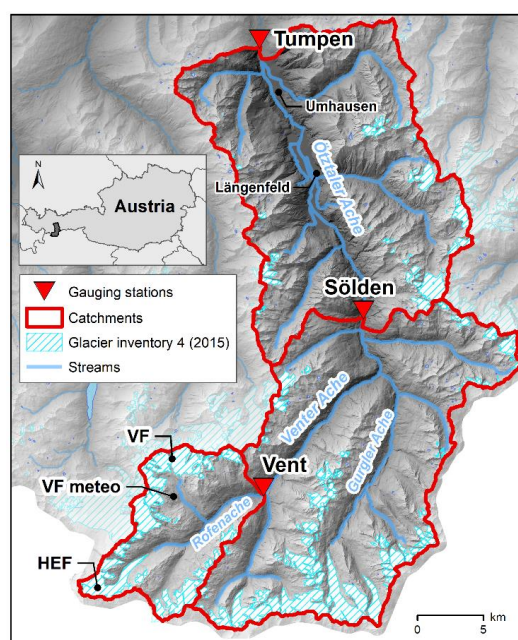
Figure 1: Nested catchment areas of the three gauging stations Vent, Sölden and Tumpen within the Upper Ötztal, Tyrol, Austria. The locations of the Hintereisferner and Vernagtferner glaciers are marked by HEF and VF, respectively. 'VF meteo' shows the location of the Vernagtferner meteorological station (Bavarian Academy of Sciences and Humanities) providing precipitation and air temperature data for the event analysis. Sources: 10 m DTM of Tyrol (Land Tirol, 2016), Glacier inventory 4, 2015 (Buckel and Otto, 2018), rivers and water bodies by tiris.ogd, Hydrography, State of Tyrol.

The climate in the catchment is comparatively dry since it is located in the inner Alpine region and is shielded from precipitation arriving from both the North and the South (Kuhn et al., 1982). Annual precipitation recorded at valley stations such as Vent (687 mm) or Längenfeld (see Fig.1, 730 mm) (Hydrographic yearbook of Austria, 2016) are much lower than recordings by accumulating rain gauges in altitudes >3000 m, where annual precipitation can exceed 1500 mm (Kuhn et al., 2016; Strasser et al., 2018). The precipitation gradient with elevation has been estimated at about 5% per 100 m (Schöber et al., 2014). Mean annual temperature at the gauge in Vent is 2.5

115   °C (Strasser et al., 2018) and increases to 6.3°C at Umhausen (see Fig. 1), 5 km upstream of the Tumpen gauge (ZAMG, 2013).

The Ötztaler Ache is one of the largest tributaries of the Inn River and is fed by the Venter Ache and Gurgler Ache (Gattermayr, 2013). Upstream of Tumpen, the Ötztaler Ache is largely uninfluenced by hydropower, with few small hydroelectric plants upstream of gauge Sölden and Tumpen that do not retain water and temporarily store

120   coarse sediment fractions in sand traps. The Ötztaler Ache shows a strong seasonality with a snow and ice melt dominated peak in summer (e.g. Strasser et al., 2018) and low-flow conditions in winter.

All sub-catchments are partially glaciated, ranging from almost 28% glacier cover in the Vent catchment to 10 % glacier cover in the Tumpen catchment (Table 1). Glaciers in the area are subject to accelerating glacier retreat, as can be seen in the difference between the two glacier inventories 3 and 4 from 2006 and 2015 (Buckel and Otto,

125   2018; Fischer et al., 2015)(Table 1). The magnitude of this glacier retreat is illustrated in the reduction in glacier cover from almost 35 % in 2006 to 28 % in 2015 in the Vent catchment. With respect to land cover, high elevations are dominated by glaciers and bare rock or sparsely vegetated terrain while lower altitudes are characterized by mountain pastures and coniferous forests as well as agriculture in the valley floors. The mean slope decreases from Tumpen to Vent.

130

Table 1: Characteristics of the sub-catchments. Calculations based on: 1) DTM of Tyrol, 10m resolution (Umweltbundesamt, 2018), 2) Glacier inventory 3 (Fischer et al., 2015) and 3) Glacier inventory 4 (Buckel and Otto, 2018) using ArcGIS Version 10.6.1.

Catchment	Vent (V)	S-V	Sölden (S)	T-S	Tumpen (T)
Catchment size [km²] [1]	98.1	342.7	440.8	342.0	782.8
Mean elevation (min - max) [m.a.s.l.] [1]	2891 (1891 - 3772)	2607 (1343 - 3619)	2670 (1343 - 3772)	2250 (931 - 3496)	2487 (931 - 3772)
Mean slope (min – max) [°][1]	25 (0 - 76)	29 (0 - 83)	28 (0 - 83)	32 (0 - 83)	30 (0 - 83)
Glacier cover GI 3 (2006) [%] [2]	34.4	14.8	19.2	4.9	12.9
Glacier cover GI 4 (2015) [%] [3]	28.1	11.9	15.6	3.6	10.3
Glacier cover GI 3 (2006) [km²] [2]	33.7	50.8	84.5	16.8	101.3
Glacier cover GI 4 (2015) [km²] [3]	27.6	41.0	68.6	12.4	81.0

135

2.2. Data and analyses
2.2.1.   Discharge and sediment concentration data

For our analyses, we used discharge and turbidity-based suspended sediment concentration data from the three gauging stations Vent (Rofenache), Sölden and Tumpen as depicted in Fig. 1 (Table 2).

140   Although discharge data have been recorded by the Hydrographic Service of Tyrol since 1967 and 1976 in Vent and Tumpen, respectively, we only considered the period of time when concomitant turbidity measurements are available i.e. since 2006. This was to focus on analyzing the present and recent past and to exclude long-term trends e.g. due to increased glacier ablation since the 1980s (Hock, 2020) as much as possible.

Sediment concentration data at all stations are acquired by continuous turbidity measurements using optical infra-

145   red turbidity sensors. At the gauges in Vent and Tumpen, water samples are taken by hand close to the turbidity probes in the stream and at several points spanning the width of the gauge for calibration to sediment concentrations (for details see Lalk et al., 2014).

Table 2: Characteristics and sources of investigated data (HD = Hydrographic Service of Tyrol, Austria; TiWAG = Tiroler Wasserkraft AG/Hydropower company of Tyrol). Data of the Hydrographic Service of Tyrol of 2019 and 2020 are preliminary. *Turbidity measurements in Vent and Sölden are interrupted during the winter months to prevent damage to the equipment by ice.

150

Station	Variable	Temporal resolution	Spatial resolution	Time period	Source
Vent (Rofenache)	Discharge	15 Minutes	Gauge measurement	2006 - 2020	HD
	Suspended sediment concentrations*	15 Minutes	Gauge measurement	2006 - 2020	HD
Sölden	Discharge	15 Minutes	Gauge measurement	2012 - 2020	TiWAG
	Suspended sediment concentrations*	15 Minutes	Gauge measurement	2012 – 2020 (2018 missing)	TiWAG
Tumpen	Discharge	15 Minutes	Gauge measurement	2006 - 2020	HD
	Suspended sediment concentrations	15 Minutes	Gauge measurement	2006 - 2020	HD
All catchments	Snow cover	daily	250 m	2002 - 2018	Matiu et al., 2020

Similarly, at the gauge in Sölden, water samples taken close to the turbidity sensor were used to translate turbidity

155 measurements into a continuous sedigraph from 2012 to 2017 (see Schöber and Hofer, 2018, for details). We took

additional water samples in Sölden in 2019 and 2020 using automatic samplers in order to improve the data situation especially at rarely sampled high concentrations and to continue observations as measurements by the TiWAG had been discontinued after 2017. For this purpose, the turbidity values recorded by the turbidity probe were recorded by a logger programmed to initiate sampling if one of three criteria was met: (i) regular sampling, to ensure

160 one sample at least every four days, (ii) threshold-based sampling to obtain samples across the whole range of possible turbidity values and (iii) event-based sampling, where a sample was initiated if the rise in turbidity was exceptional as compared to the time period before. The suction tube of the automatic sampler in Sölden was attached to the turbidity sensor's case, which was immersed at the side of the channel. Gravimetric sediment concentrations SSCg were then determined in the laboratory by filtering the water samples onto glass fiber filters with

165 a pore size of 0.45 μm and drying the filters at 60°C until the weight was constant (see e.g. Delaney et al., 2018b). In total, we took 99 samples in Sölden between April 2019 and October 2020. To verify whether these can be combined with the 268 samples taken by the TiWAG between 2012 and 2017, we tested for significant differences between linear models estimated on the two groups by means of an ANCOVA. This showed no significant differences between the two linear models. However, strictly speaking, the assumptions for an ANCOVA are violated

170 because the residuals of the TiWAG data are not normally distributed (Shapiro-Wilk test, $p < 0.001$). By contrast, the residuals of our data are normally distributed (Shapiro-Wilk test, $p = 0.03$), which allows for the computation of confidence and prediction intervals around the linear model (Fig. 2). Since all data points of the TiWAG samples are located within the prediction interval and the linear model based on TiWAG data lies within the confidence interval of the linear model based on our data, we conclude that there is a good enough agreement to estimate one

175 linear model using all 367 available samples. The resulting model (SSC = 1.8487*turbidity + 0.0079, R^2 = 0.84) is applied to the complete turbidity time series.

The variance observed in the SSC-turbidity relationship does not appear to be unusually high compared to other studies reporting similar coefficients of determination (Delaney et al., 2018b; Felix et al., 2018) and can be attributed to changes in particle size, shape or color (Merten et al., 2014).
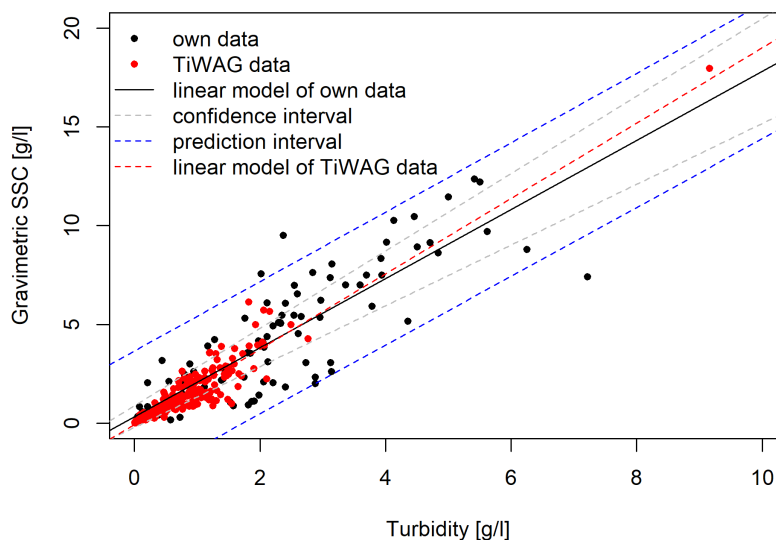
180

Figure 2: Gravimetric suspended sediment concentrations in samples vs. turbidity measured at gauge Sölden: TiWAG samples taken between 2012 and 2017 are all located within the prediction interval of the linear regression based on our samples and the linear model based on TiWAG data is located within the confidence interval.

185 **2.2.2. Sediment event analysis**

To assess the relative importance of sediment events in time and space, we analyzed the largest suspended sediment flux events of each year in Vent and Tumpen. We excluded Sölden from the analysis, as comparability would be limited since data are missing before 2012 and in 2018.

For the Vent catchment, we analyzed the events with respect to the antecedent air temperature and precipitation

190 conditions. Since availability of high-quality (i.e. gap-free) data in high temporal resolution is limited, we confined this analysis to the years 2011 to 2020. We based our analysis on discharge and sediment concentration data of the Vent gauge and precipitation and air temperature data of the Vernagtferner station (2640 m a.s.l., located 6.25 km west of the gauge in Vent within the catchment) provided by the Bavarian Academy of Sciences. We visually identified suspended sediment flux (SSF) peaks that were clearly higher than the characteristic daily amplitude of

195 the respective season i.e. the days before and after. In order to be classified as a precipitation event, precipitation had to be > 3 mm in the 24 hours ahead of the end of the event. While this might seem like very little precipitation to become erosive, it has to be considered that precipitation can vary greatly within the almost 100 km² catchment. Therefore, we considered the hydrograph shape as additional indication, which typically shows a sharp increase in case of a precipitation event. For classification as a melt-induced event, liquid precipitation had to be smaller

200 than 3 mm within 24 hours and the mean absolute temperature had to be above 0°C. Additionally, we considered temporal development in daily snow cover data (Sect. 2.2.3) for the verification of snowmelt events. We determined the beginning and end of the events visually. In this, we aimed for the beginning of the rising limb and the return to the before-event level of sediment flux or the point of inflection before the next event or daily fluctuation. As a result, we chose to count two adjacent peaks as two events and possibly cut off long tails of events, e.g. if

205 mass movements lead to elevated sediment fluxes for a longer period.

For the Tumpen catchment, we visually identified SSY peaks as described above for the years 2011 to 2020 to ensure comparability. However, given the almost 800 km² area of the Tumpen catchment with considerable topography, there are only few stations measuring precipitation for the whole time and in sufficient temporal (i.e. sub-daily and preferably sub-hourly) resolution. Therefore we did not classify the events with respect to precipitation events.

2.2.3. GIS analysis, snow cover data and statistical analyses

To derive the catchment areas for the three gauges, we used ArcGIS (version 10.6.1) and the 10 m Digital Terrain Model of Tyrol (Land Tirol, 2016) to calculate the flow direction (D8) and flow accumulation and finally used the watershed tool. We then clipped the glacier areas of the glacier inventory 3 (Fischer et al., 2015) and 4 (Buckel and Otto, 2018) with the resulting catchment areas to obtain the respective glacier areas within the catchment (Table 1) and erased the areas of glacier inventory 4 of 2015 from the inventory 3 of 2006 to assess recently deglaciated areas.

In order to analyze land cover classes within the different elevation bands, we first calculated 250 m elevation bands for the whole catchment area upstream of gauge Tumpen using the contour tool. Subsequently, we clipped glacier inventories and CORINE land cover data (Umweltbundesamt, 2018) to the elevation band areas.

We calculated average weekly snow free areas based on data provided by Matiu et al. (2020), who used MODIS remote sensing products and derived daily nearly cloud-free snow cover data for the European Alps using temporal and spatial filters. We used these gridded data and intersected them with the areas of the 250 m elevation bands to gain the daily percentages of snow free area for each elevation band and averaged these for each week of the year. In this, our basic idea is similar to the active contributing drainage area (ACDA) as proposed by Li et al. (2021), which uses the freezing line altitude to quantify the percentage of the catchment where the ground is unfrozen and thus susceptible to erosion. However, as an advantage to the ACDA, which yields the percentage of unfrozen area for the whole catchment, we are able to differentiate between different areas within the catchment. We consider the resulting snow free fraction of the respective elevation bands as potentially erodible under the assumption that the ground no longer covered by snow is largely unfrozen and thus susceptible to erosion.

All statistical analyses were conducted in R version 3.5.1 (R Core Team, 2018). In order to assess discharge and sediment flux seasonality, we calculated weekly Pardé-coefficients (i.e. the ratio of the average weekly discharge to the average annual discharge) and the average percentage of annual suspended sediment loads transported in a given week of year.

3   Results
3.1.   The Vent catchment has the highest mean annual discharge and suspended sediment yields

To compare discharge and suspended sediment yields in space, we calculated specific values (i.e. per unit area) for the catchments above the gauges Vent, Sölden and Tumpen, but also for the areas in between the gauges: e.g. the intermediate catchment S-V refers to the area within the Sölden catchment excluding the catchment upstream of gauge Vent (Fig. 3).
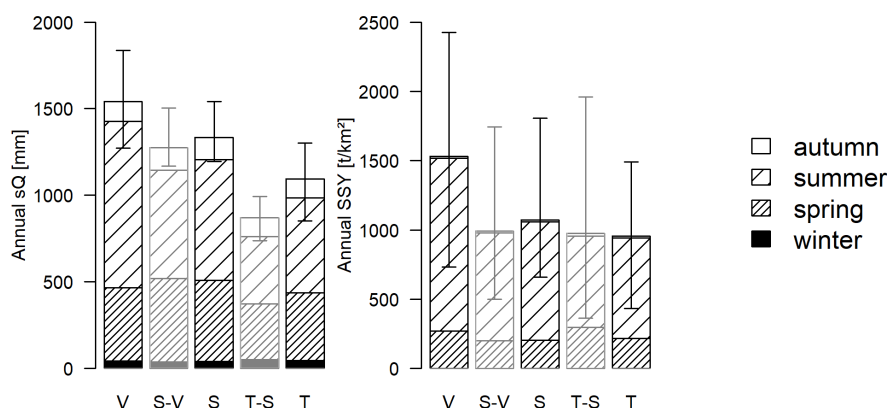
245 **Figure 3: Mean annual specific discharge (sQ) and suspended sediment yields (SSY) are highest at the gauges Vent as compared to Sölden and Tumpen and the intermediate catchments between gauges Vent and Sölden (S-V) and Sölden and Tumpen (T-S). Bars are divided into seasons: winter (Jan – Mar), spring (Apr – Jun), summer (Jul – Sep), autumn (Oct – Dec). Whiskers depict minimum and maximum annual values.**

Mean annual discharge per area (sQ) are highest in the Vent catchment with 1543 mm/a, and gradually decrease

250 to 885 mm/a in the T-S catchment, i.e. the area between the lowest gauge in Tumpen and the gauge in Sölden.

Suspended sediment yields (SSY) are markedly higher in the Vent catchment (1532 t/km² per year on average) as

compared to Sölden and Tumpen (1071 and 954 t/km² on average) and the intermediate catchments. Adding to

this, SSY show much higher interannual variability than sQ and the variability is highest at the gauge in Vent.

Remarkably, the specific discharge in the order of 1500 mm at the gauge in Vent seems unusually high compared

255 to areal precipitation estimates for the Vent catchment between 1200 and 1500 (Hanzer et al., 2018; Kuhn et al.,

2016; Stoll et al., 2020), leaving almost no room for evapotranspiration. However, this is due to the contribution

of non-equilibrium glacier melt and thus release of water from the long-term glacier storage (Hock et al., 2005).

Absolute mean annual discharge and sediment loads increase with increasing catchment size (Table 3). The dis-

tributions of both fluxes are severely right-skewed (as the location of mean to maximum values show) since low

260 values are much more frequent than high values. Maximum sediment concentrations decrease slightly with in-

creasing catchment size, which points to a dampening along the flow-path.

Table 3: Mean (Min - Max) observed values of discharge (Q), suspended sediment concentrations (SSC) and suspended sediment loads (SSL) at the three gauges. For better comparability between the stations, SSC recorded during the winter months from November to April were set to zero if there were NA values.

Station	Q [m³/s] mean (min-max)	SSC [g/l] mean (min-max)	SSL [10³ t/year] mean (min-max)
Vent	4.8	0.54	150.3
(2006 – 2020)	(0.1 – 76.3)	(0 – 59.2)	(72.0 – 238.0)
Sölden	19.2	0.59	472.3
(2012 – 2020)	(0.9 – 247.6)	(0 – 49.2)	(291.3 – 797.0)
Tumpen	27.2	0.60	747.6
(2006 – 2020)	(2.7 – 266.2)	(0 – 50.7)	(339.8 – 1167.8)

3.2. Differences during the glacier melt period account for most of the differences in mean annual Q and SSY

To investigate whether the spatial differences of mean annual fluxes are equally distributed across the seasons, we subdivided the year into seasons that match governing hydrological processes, so that "spring" from April to June corresponds to the time dominated by snowmelt and "summer" from July to September corresponds to the bulk of glacier melt (Fig. 3).

Both discharge and suspended sediment fluxes are not equally distributed throughout the year. The discharge regimes at all gauges are clearly dominated by spring and summer streamflow (April – September), whereas autumn and winter discharge contributions (October – March) are small and almost equal across all sub-catchments. The most striking differences between the sub-catchments occur during the glacier melt period in summer, when specific discharge in the Vent catchment is markedly higher than in the downstream catchments.

Sediment fluxes are even more seasonal than discharge, with almost no transport during autumn and winter (October – March). Mean summer SSY are markedly higher in Vent (1200 t/km² per year) than in the other catchments (660 – 860 t/km² per year) and differences between the sub-catchments are less pronounced in spring (ranging from 200 t/km² in the S-V to 300 t/km² in the T-S sub-catchment).

It has to be noted, that there are no turbidity measurements and resulting suspended sediment concentrations at the Vent and Sölden gauges during late autumn and winter to prevent damage to the equipment. However, turbidity recordings at the Tumpen gauge show that the total SSY of roughly 0.5 t/km² in January to March accounts for less than 1% of the annual SSY and is thus negligible compared to the rest of the year. Furthermore, the equipment in Vent and Sölden is reinstalled before the initial rise in concentrations in spring.

3.3. Mean annual discharge and suspended sediment fluxes correlate positively to glacier cover

Annual specific discharge (sQ) and suspended sediment yields (SSY) show significant positive correlations ($\alpha = 0.001$) with increasing glacier cover in the respective catchments, although the high interannual variation in SSY leads to a much weaker relationship and lower R^2 than for sQ (Fig. 4).
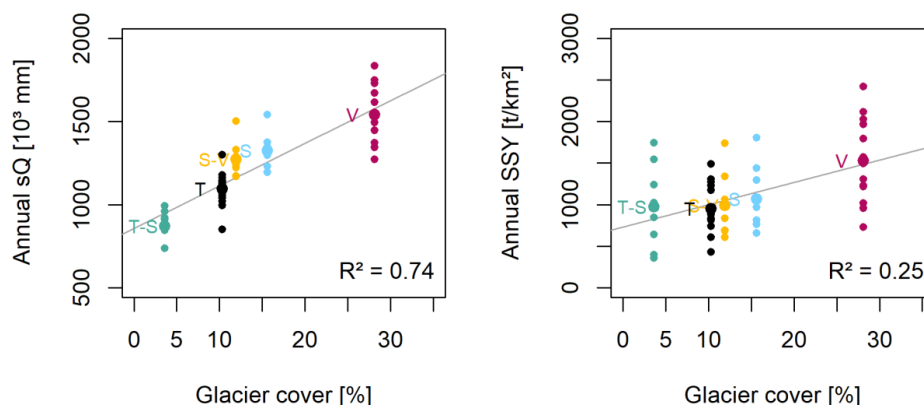
Figure 4: Annual specific discharge (left) and annual suspended sediment yields (right) increase with increasing glacier cover (glacier inventory 4, 2015; Buckel and Otto, 2018) in the sub-catchments

Specific discharge increases with increasing glacier cover because glacier storage is not in equilibrium and glacier melt water contributes a large part to the annual discharge (Kuhn et al., 2016). For example, the annual mass

balances of the Vernagtferner and Hintereisferner within the Vent catchment have been negative since the 1980s

300 and their mean annual mass balances in the years 2005/06 to 2017/18 amounted to -909 and -1243 mm water

equivalent (World Glacier Monitoring Service, 2021). (Please note that these values are calculated relative to the

respective glacier area and are thus not directly comparable to catchment precipitation or discharge.)

However, precipitation also increases with elevation. The mean annual precipitation recorded close to the Vent

gauge is 666 mm while areal precipitation of the whole catchment is estimated between 1200 and 1500 mm, and

305 for the 11.4 km² Vernagtferner sub-catchment (featuring 74 % glaciation and an elevation range of 2600 – 3600

m), even 1525 to 1900 mm are reported (Braun et al., 2007; Hanzer et al., 2018; Kuhn et al., 2016; Stoll et al.,

2020).

3.4. Annual discharge and sediment yields correlate positively to annual glacier mass balances within

310 the Vent catchment

As mentioned above, the interannual variability in sediment yields is much higher than for discharge. While min-

imum and maximum annual discharge volumes at the three gauges differed by a factor of 1.3 to 1.5 in the years

2006 to 2020, sediment yields varied by a factor of 3.3 to 5.4 (see also whiskers in Fig. 3 or the range of values at

each gauge in Fig. 4 and 5). In both variables, the variability was most pronounced at the highest gauge in Vent.

315 In order to examine this, we considered the relationship between annual discharge and annual suspended sediment

yields as well as the relationship of both to annual glacier balances. Unfortunately, we had to limit the latter anal-

ysis to the Vent catchment as mass balance data for glaciers within the other sub-catchments are lacking.

We did not find a clear relationship of annual discharge volumes and annual sediment loads at any of the gauges

(Fig. 5), and conclude that annual discharge volumes do not seem to explain much of the interannual variability in

320 SSY.
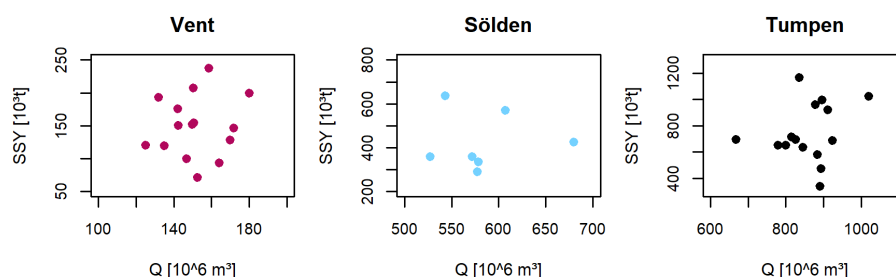
**Figure 5: Annual suspended sediment loads and discharge volumes at the gauges in Vent (left), Sölden (center) and
Tumpen (right) do not reveal a clear relationship.**

However, the interannual variability in SSY and sQ can be at least partly be attributed to differences in glacier

325 mass balances: Both variables in Vent correlate positively with the cumulative annual mass balances of Vernagt-

and Hintereisferner (Fig. 6), the two largest glaciers within the Vent catchment. Although the correlation for the

entire available discharge and mass balance time series since 1976 (grey line in left panel of Fig. 6) is significant

($\alpha = 0.01$), the correlation for the years since 2006 (i.e. the period of time investigated in this paper) is not signif-

icant and has a very low R². We attribute this to the leverage of individual years such as 2014, when a ca. 10-year

330 flood occurred in the Ötztaler Ache on August 13th and the percentage of the annual discharge during precipitation

events was 9% (the highest percentage of the 10 years examined, see Fig. 6) while the annual balance was unusually close to zero. The correlation between SSY and annual balances is significant at a level of $\alpha = 0.05$.
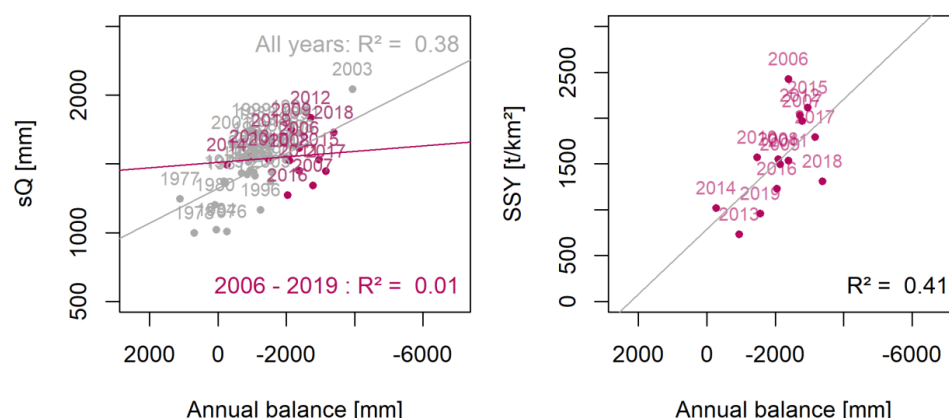
Figure 6: Annual discharge and suspended sediment yields at the gauge in Vent correlate positively to the sum of annual mass balances of the two largest glaciers within the Vent catchment Vernagtferner and Hintereisferner (World Glacier Monitoring Service, 2021) in mm, corresponding to the respective glacier areas. Grey points, line and R² in the left panel refer to the entire available discharge and mass balance time series starting in 1976.

3.5. Discharge and sediment fluxes show distinct seasonalities in all sub-catchments and sediment fluxes are constrained to a shorter period of time

In order to assess discharge and sediment flux seasonality across spatial scales, we calculated weekly Pardé-coefficients and the percentage of suspended sediment loads transported in a given week of year (Fig. 7).

Discharge volumes are very low between October and March at all gauges due to temperatures below the freezing point. As temperatures start to rise in spring, snowmelt usually starts around March in low elevations and mid-May in high elevations (see also Fig. 8) causing the initial increases in discharge. In June, snowmelt can contribute up to 80 % of the total discharge volumes in the Vent catchment (Schmieder et al., 2018). Glacier melt starts in June and peaks in July and August when large glacier areas are snow free, with peak shares of the total discharge volumes of 75 % on individual days (Schmieder et al., 2018) before receding as temperatures drop in September or October (see also Kormann et al., 2016). Adding to this, precipitation shows a certain (albeit less pronounced) seasonality, with a maximum of average monthly precipitation in July (79 mm) and minimum in February (32 mm) as calculated from daily recordings in Vent since 1935 (Stoll et al., 2020).

The seasonality of suspended sediment yields is even more pronounced than in discharge as sediment fluxes start to increase later in the year and decrease earlier than discharge, and are thus constrained to a smaller time window at all gauges (Fig. 7). The highest weekly contributions to annual yields occur during the ice-melt dominated period after mid-July, coinciding with the highest weekly Pardé-coefficients at the highest gauge Vent but delayed with respect to the highest Pardé-coefficients at the lower-lying gauges (Fig. 7).

Earth **Surface**
Dynamics
Discussions
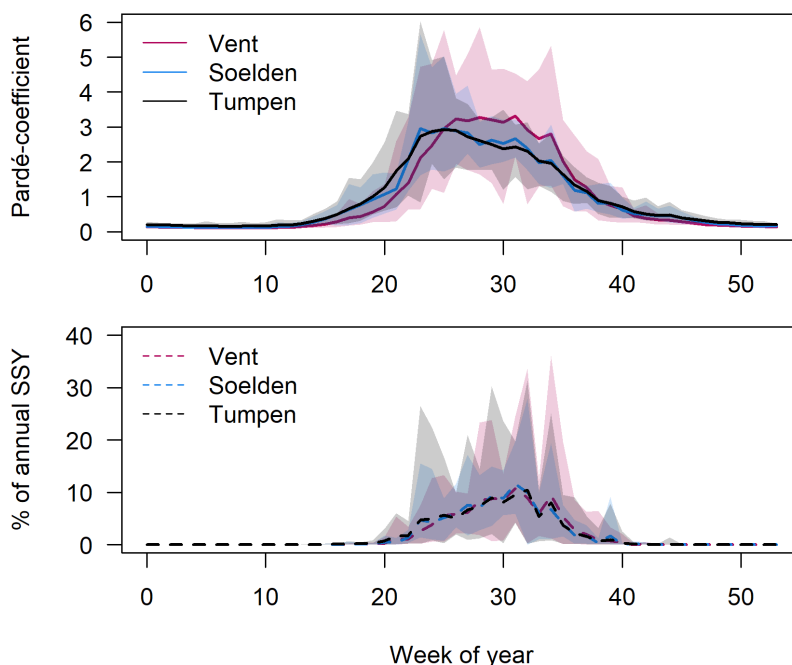
Figure 7: Distinct seasonality illustrated by Pardé-coefficients (ratio of average weekly discharge to average annual discharge) and percentages of annual SSY fluxes in weekly resolution. Lightly colored areas show minimum and maximum values of individual years.

3.6. Discharge seasonality changes in space – but sediment seasonality occurs simultaneously at the three gauges

Discharge seasonality becomes more pronounced with elevation (Fig. 7): Of the annual runoff, 62%, 52% and 50% are generated in summer in Vent, Sölden and Tumpen, and 11%, 13% and 14% in winter and autumn, respectively. Thus in lower elevations, discharge volumes are more evenly distributed throughout the year due to shorter snow cover periods, a less important contribution of glacier melt and larger relative contributions of precipitation (Kormann et al., 2016). An analysis of the individual years showed that the timing of the discharge increase in early spring is very similar in the three gauges. However, the specific discharge initially is lower in Vent as compared to Sölden and Tumpen, as snowmelt starts roughly at the same time in spring in all sub-catchments, but at a much lower rate upstream as compared to downstream as temperatures above the freezing point occur earlier in lower areas. Later in summer, specific discharge is higher in Vent as compared to Sölden and Tumpen. This is likely due to the higher proportion of glaciation further upstream and associated higher daily discharge maxima during summer (Gattermayr, 2013) as well as the aforementioned higher precipitation in higher elevations which directly contributes to discharge as it does not fall as snow during this time.

Interestingly, the timing and seasonal distribution of specific sediment yields are very similar at the three gauges (Fig. 7), although absolute sediment loads are higher at the downstream gauges. This was also confirmed by an analysis of individual years: Only in four of the 15 years of data (2007, 2009, 2018 and 2019), very small portions of the annual yield in Tumpen were transported starting two weeks before the initial rise in Vent, but the first sharp increase in SSY was always simultaneous at the three gauges. The suspended sediment seasonality changes only

slightly with elevation: 81%, 80% and 76% of the annual SSY are transported in summer in Vent, Sölden and Tumpen and 18%, 19% and 23% in spring, respectively. The striking decrease in SSY at all stations in week 33 (i.e. around mid-August) is due to the coincidental absence of large events in the observed period in this week as compared to the weeks before and after.

385

3.7. Sediment flux onset in spring coincides with snow melt above 2500 m a.s.l.

To explore the simultaneous onset of sediment fluxes and the delay compared to the initial rises in discharge, we used a synoptic view of the mean spatiotemporal snow cover evolution with sediment seasonality.
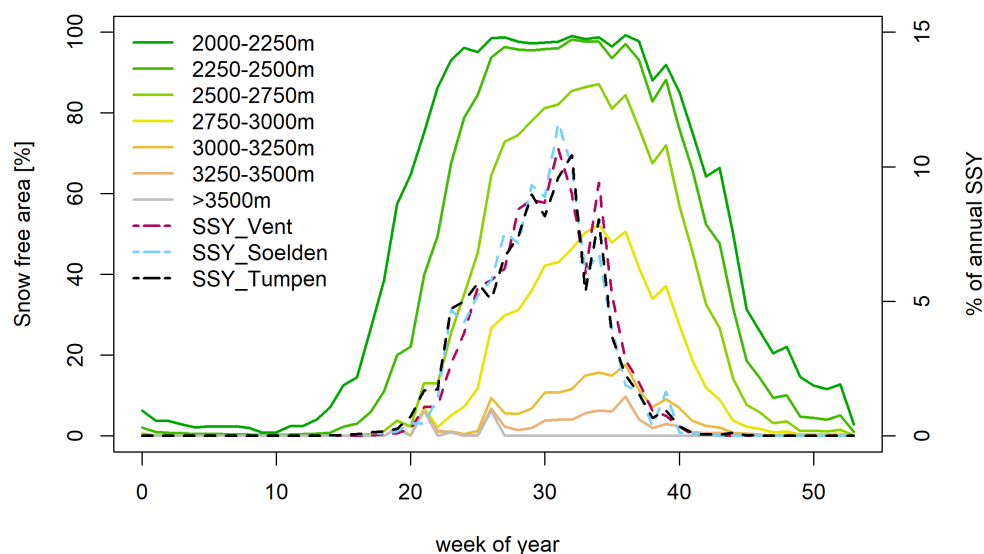
Figure 8: The spring increase in mean weekly percentage of annual suspended sediment yields coincides with the increase in mean weekly snow free fraction of the areas above 2500 m a.s.l. within the Tumpen catchment.

The spatial snow cover evolution shows that in March (ca. week 10), the entire area above 2000 m is usually covered by snow (Fig. 8). Until the end of April (ca. week 18), the area above 2500 m is still entirely snow covered while about 20% and 60% of the two elevation bands below 2500 m are already snow-free. Starting in May, snow melts in areas above 2750m. This is well in accordance with snow melt timing in the Vent catchment as reported by (Kuhn et al., 2016).

The initial rise in suspended sediment fluxes at all gauges coincides with the onset of snowmelt above 2500 m. Further differentiation between the elevation bands above 2500 m is difficult: firstly, an analysis of the individual years showed that snowmelt often started simultaneous in all elevation bands above 2500 m (although with different intensities). Furthermore, (Matiu et al., 2020) warn against too detailed analyses of short periods of time due to uncertainties in the snow cover data and advise to average over weeks to months. Yet what was clear from the analysis of individual years as well as from Fig. 7 is that the onset of snowpack removal in the areas below 2500 m always preceded the initial rise in suspended sediment fluxes at the three gauges.

In autumn, sediment transport declines as soon as the first snow cover starts to build up, which happens simultaneously at all elevations above 2000 m but to variable extents. This concurrence supports the suitability of the

snow-free fraction as a proxy for susceptibility to erosion: as soon as snow remains on the ground, temperatures must be below the freezing point so that precipitation falls as snow and does not lead to erosion, frozen surfaces are no longer erodible and at the same time, surface runoff and glacier melt decreases.

410

3.8.   The areas above 2500 m include glacier tongues, bare rock and the lowest parts of the most recently deglaciated areas

To investigate if the co-occurrence of snowmelt above 2500 m with spring increases in sediment transport is linked to changes in land cover, we analyzed CORINE land cover data for the individual elevation bands (Fig. 9). The most striking differences between the areas below and above 2500 m a.s.l. are the decrease in natural grasslands and the increase in bare rock surfaces. Moreover, the first glacier areas can be found above 2500 m and for most glaciers in the area, the (tip of the) glacier tongue is located here. In the elevation band below, between 2250 and 2500 m a.s.l., 93% of the 0.5 km² glacier area that had remained in this elevation band during the glacier inventory of 2006 had melted until 2015. Thus the most recently deglaciated proglacial zones – with a much larger area of 3.2 km² glacier retreat between 2006 and 2015 – are located between 2500 and 2750 m, uncovering large amounts of glacially conditioned sediment.
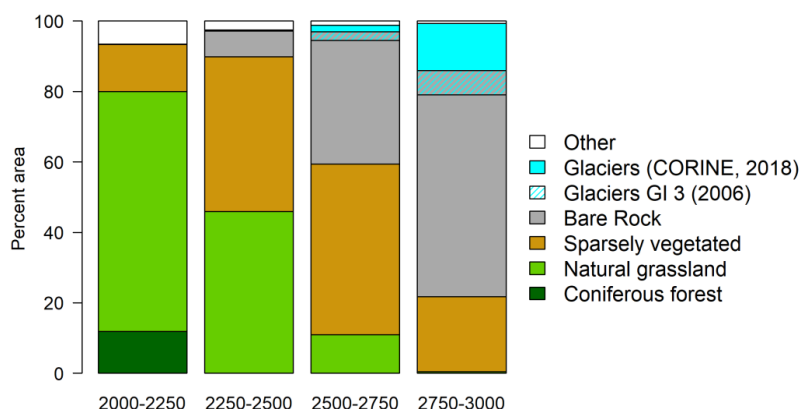
Figure 9: Land cover in the elevation bands between 2000 and 3000 m a.s.l. based on CORINE land cover data (Umweltbundesamt, 2018)

425

3.9.   Individual events account for a higher share of sediment fluxes compared to discharge and their relative importance is similar in Vent and Tumpen

To compare the relative importance of events in space, we visually identified the strongest sediment flux events of each year from 2011 to 2020 in Vent and Tumpen and analyzed the discharge and sediment fluxes during these

430 events.

For Vent, we identified between 6 and 16 events per year and a total of 100 events. Of the counted events, 95% were shorter than 24 hours and the periods classified as events correspond to 0.5 to 1.5 % of the year. All events combined transported on average 7% of the annual discharge (min. 4% - max. 9 %, i.e. 6*106 to 13*106 m³) and 25 % of the annual sediment yield in Vent (min. 12% – max. 40%, i.e. 8.5*103 to 57*103 t).

435 In Tumpen, we identified between 7 and 13 events per year and a total of 84 events. Compared to the 100 events identified in Vent, this means that some of the events detected in Vent did not stand out against the diurnal amplitude in Tumpen. The events in Tumpen were slightly longer than the events in Vent, as only 83 % were shorter than 24 hours. All events combined on average accounted for 6 % of the annual discharge (between 4 and 9 % of the annual discharge, i.e. 35*106 and 80*106 m³) and 26 % of the annual SSY in Tumpen (min. 16 % to max.

440 38%, i.e. 102*103 t to 372*103 t). Similar to Vent, the periods classified as events correspond to 1 to 2 % of the year.

Although we only examined the events of the last 10 years, these proportions seem to be representative for the whole time series since 2006, as indicated by the grey area in Fig. 10, which shows that up to almost 40 % of the cumulated yield is transported within 2 % of the time. Thus, the fluxes during events can be very relevant for

445 overall sediment dynamics, but are less important for discharge. In combination with the more pronounced seasonality of sediment fluxes, this explains the much "flashier" behavior as compared to discharge (Fig. 10).
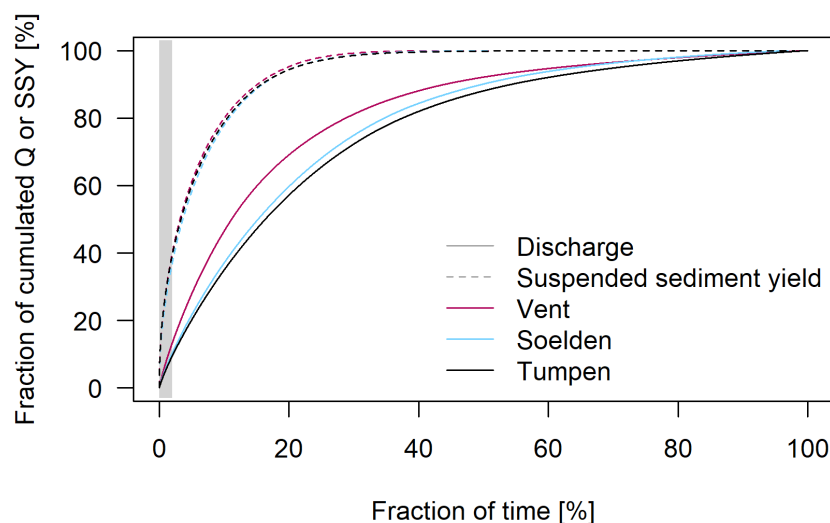
Figure 10: Duration curves of Q and SSY based on 15-minute data. The grey area indicates 0 - 2 % of the time and represents the time classified as events. Note that the three lines for suspended sediment yields are very similar and
450 **might appear as if it was only one line.**

3.10. Peak sediment fluxes and concentrations are associated with (precipitation) events, but the bulk of discharge and sediment fluxes are thermally induced

To pinpoint the dominant processes on the sub-seasonal scale, we analyzed how important precipitation events

455 were for sediment dynamics as compared to thermally induced flux events, i.e. snow or glacier melt. For this purpose, we analyzed sediment events with respect to the antecedent temperature, precipitation and snow cover conditions. We focused this analysis on the highest catchment in Vent and to the years 2011 to 2020 due to the limited availability of long (quasi) gap-free precipitation time series in high temporal resolution.

Of the identified Events, 84% were associated with precipitation while the remaining events were associated with

460 the melting of snow or ice. The events associated with precipitation transported on average 21% (min. 7% - max. 40 %) of the annual SSY and 5% (min. 2% - max. 9%) of the annual discharge. The most extreme event was observed in August 2014, when 26% of the annual SSL (ca. 26 000 t) and 2.2% of the annual discharge were transported in only 25 hours. We hypothesize that this was associated with mass movements, as the event was

preceded by a prolonged precipitation period (67 mm within 7 days and 30 mm within 24 hours before the event),
yet do not have field observations from this time.

However, we did observe an event on August 28th 2020, when an extreme precipitation event of about 100 mm
within 3 days lead to a mass wasting event onto the Hintereisferner, one of the largest glaciers within the Vent
catchment. Thirteen percent of the total annual suspended sediment load at gauge Vent (about 15 000 t) were
exported within the first 30 hours and 20% within four days. The starting zone of the observed mass movement is
located in an area with a high probability of permafrost occurrence (Boeckli et al., 2012).

4   Discussion

The aim of the present study was to pinpoint the areas and processes most relevant to discharge and sediment
dynamics on several spatial and temporal scales in the Ötztal. To our knowledge, it represents the first study using
a nested catchment setup and investigating several temporal scales in a glacierized, alpine setting.

Firstly, this approach allowed us to determine the order of magnitude of mean annual discharge and suspended
sediment yields (SSY) on several spatial scales of 900 to 1500 mm for discharge and 1000 to 1500 t/km² for SSY,
which generally correspond well to values reported for more catchments in the Ötztal and Stubai Alps (Schöber
and Hofer, 2018). SSY fall at the high end compared to the extensive collection of studies compiled by Hinderer
et al. (2013) for the European Alps: only three catchments (the Haut Glacier D'Arolla and, the Tsidjiore Nouve
and the Vispa with higher or similar glacier covers as compared to Vent), showed higher annual SSY than at the
gauge Vent.

Secondly, we found that mean annual values for both Q and SSY correlate positively with glacier area. Similar
correlations have been reported across the European Alps (Hinderer et al., 2013; Lalk et al., 2014; Schöber and
Hofer, 2018) and now this relationship has been demonstrated for a setting of nested catchments. The increase of
discharge with glacier cover is reasonable given the higher contribution of glacier meltwater in Vent as compared
to lower elevations, where snowmelt gains in relative importance (Kormann et al., 2016; Weber and Prasch, 2016).
Further contributing factors are higher precipitation amounts in higher elevations due to the considerable precipi-
tation gradient (about 5 % per 100m, Schöber et al., 2014) and lower temperatures and vegetation cover leading
to lower evapotranspiration. The increase of SSY with glacier cover is in line with the current understanding that
glaciers act as important sediment sources, especially during the transitional, paraglacial state of deglatiation (Bal-
lantyne, 2002), through glacial erosion, the provision of proglacial sediments following their retreat and the
transport of subglacial sediments by meltwaters (Beylich et al., 2017; Delaney et al., 2018a; Schöber and Hofer,
2018). This is further supported by the positive correlation between annual glacier mass balances and SSY as well
as our finding that differences in mean annual Q and SSY were mainly due to differences during the glacier melt
period. Interestingly, specific discharge volumes show much lower interannual variability than suspended sedi-
ment yields, which we account to the compensating effect of glaciers for interannual streamflow variability (Hock
et al., 2005).

We further assessed the spatio-temporal distribution through analyzing the seasonality of both fluxes at the three
gauges. This showed that discharge seasonality is scale-dependent, as discharge increases earlier at the lower
gauges due to earlier onsets of snowmelt in lower elevations (see also Kormann et al., 2016, Weber and Prasch,
2016). Accordingly, the highest weekly Pardé-coefficients are observed during the snowmelt phase at the gauges
Sölden and Tumpen but during the glacier melt phase in Vent.

In contrast, SSY seasonality is synchronous at the three gauges and sediment transport seems to be limited in spring as the initial rise in discharge volumes precedes the beginning of sediment transport and similar discharge volumes transport higher sediment fluxes in late summer as compared to spring. We concluded that areas above 2500 m are crucial source areas from the co-occurrence of the spring increase in sediment seasonality at all three gauges with snowmelt above 2500 m a.s.l., under the assumption that areas are unfrozen and erodible after snow-pack removal. The areas above 2500 m contain landscape elements such as glacier tongues and proglacial areas which have been identified as very significant for sediment dynamics in other catchments (Delaney et al., 2018a; Orwin and Smart, 2004; Schöber and Hofer, 2018). For example, Delaney et al. (2018a) found that although far more sediment originated subglacially, erosion rates in proglacial areas were over 50 times greater than in the rest of the Griesgletscher catchment in the Swiss Alps.

As another characteristic of the areas above 2500 m, permafrost is likely to occur in favorable or cold conditions according to the permafrost distribution map provided by Boeckli et al. (2012) and as demonstrated by Klug et al. (2017). Thus, erosion processes associated with permafrost thawing could also play a role, as for example the active layer becomes susceptible to pluvial erosion once it has thawed (Li et al., 2021), although these processes probably do not take effect before the end of the snowmelt period. Still, assuming that permafrost degradation is an ongoing and largely irreversible process, the increase of erodible surfaces in this elevation band due to perma-frost melt seems very likely.

We conclude that sediment transport in all three catchments is limited as long as the areas above 2500 m are frozen or snow-covered and subglacial sediment sources are still inactive. This has implications for the future, since these areas will likely be snow-free for longer periods in summer (Hanus et al., 2021; Hanzer et al., 2018) during which sediments from these areas can be mobilized. At the same time, the crucial areas might increase in size as glaciers retreat and recently deglaciated areas increase.

In even higher temporal resolution, we found that highest sediment concentrations and loads were associated with events, most of which were associated with precipitation. All events combined (up to 2 % of the total time frame) on average accounted for 25 and 26 % of the annual sediment yields but only 7 and 6 % of annual discharge in Vent and Tumpen. Similar proportions have been reported for other glacierized catchments (Leggat et al., 2015; Wulf et al., 2012) which suggests a greater availability and/or easier mobilization of sediments as compared to fluvial systems where up to 90% of sediment is transported during short, high-discharge events (Delaney et al., 2018b). While this implies that so far, thermally induced sediment transport through snow and glacier melt yields the biggest share of suspended sediment load, we also showed that individual summer rainstorm events can account for up to 26 % of the annual yield (ca. 26 000 t) within just over 24 hours if mass movements are involved.

We suggest that hydro-sedimentological events such as one observed in August 2020 – involving mass movements that were triggered by heavy precipitation and are probably associated with permafrost thaw – are likely to occur more frequently in the future: In view of expected future developments, such as more frequent high-intensity summer rainstorms (Giorgi et al., 2016), prolonged snow-free periods in summer during which these rainstorms can become erosive (Hanus et al., 2021; Hanzer et al., 2018), the exposure of vast amounts of sediment due to glacier retreat (Carrivick and Heckmann, 2017; Lane et al., 2017) and accelerating permafrost thaw which facili-tates more frequent slope-failure events (Savi et al., 2020), heavy precipitation events have the potential to gain in importance drastically with regard to driving sediment export.

5 Conclusion

545 Glaciated high-alpine areas are expected to change fundamentally with respect to their suspended sediment and discharge due to climate change, yet little is known on how exactly these changes propagate to sediment dynamics. To provide the basis for future studies investigating these future changes, we analyzed discharge and suspended sediment data from the recent past in a nested catchment setup in the Ötztal in Tyrol, Austria, and aimed to identify the areas, time periods and processes that are crucial for suspended sediment and discharge dynamics.

550 We showed that mean annual discharge and suspended sediment fluxes were highest in the smallest, highest, most glaciated sub-catchment above gauge Vent and that annual fluxes correlated significantly with annual glacier mass balances. This demonstrates that glaciated areas are important sediment sources and glacier meltwater contribution is high.

Discharge seasonality is more pronounced at higher elevations due to a later onset of snowmelt, higher glacier
555 melt contributions and a considerable positive precipitation gradient with elevation.

However, the onset of suspended sediment fluxes in spring occurs almost synchronous at the three gauges and the time lag compared to the spring increase in discharge points towards a limitation of sediments during this time. We analyzed sediment seasonality in synopsis with snowmelt timings in different elevation bands, which suggests that the areas above 2500 m a.s.l., including glacier tongues, bare rock surfaces and recently deglaciated areas, are
560 crucial for suspended sediment fluxes.

We showed that so far, precipitation events play a subordinate role as compared to thermally induced discharge and suspended sediment fluxes. However, we suggest that hydro-sedimentological events involving mass movements triggered by heavy precipitation and possibly permafrost thaw are likely to occur more frequently in the future. This would result in a shift in relative importance of precipitation events for sediment fluxes.

565 Our study extends the scientific knowledge on current hydro-sedimentological dynamics in glaciated high alpine areas and provides a baseline for investigations on projected future changes in hydro-sedimentological system dynamics. Such future investigations should focus on the areas above 2500 m and the role of precipitation events when addressing future changes in suspended sediment and discharge dynamics, e.g. in modelling studies.

6 Data availability

570

Discharge and suspended sediment concentration data from the gauges Vent and Tumpen recorded by the Hydrographic Service of Tyrol, Austria, as well as sediment concentrations from our samples taken in Sölden are published under DOI 10.23728/b2share.be13f43ce9bb46d8a7eedb7b56df3140.

Discharge and turbidity time series recorded by the TiWAG at the gauge in Sölden along with suspended sediment
575 concentration data in TiWAG samples can be requested via info-ausbau.kw.kaunertal@tiwag.at.

Precipitation and air temperature data recorded at the Vernagtferner hydro-meteorological station by the Bavarian Academy of Sciences and Humanities are successively made available on PANGEA and data until 2012 are already available at https://doi.pangaea.de/10.1594/PANGAEA.829530.

The DTM of Tyrol is available at https://www.data.gv.at/katalog/dataset/land-tirol_tirolgelnde (Land Tirol, 2016).
580 Land cover data are available at https://www.data.gv.at/katalog/dataset/clc2018 (Umweltbundesamt, 2018).

Glacier inventories are available at DOI 10.1594/PANGAEA.844985 (Fischer et al., 2015) and DOI 10.1594/PANGAEA.887415 (Buckel and Otto, 2018). Glacier mass balances are available at DOI 10.5904/wgms-fog-2021-05, 2021 (World Glacier Monitoring Service, 2021). Snow cover data are available via DOI 10.3390/data5010001 (Matiu et al., 2020).

585 ## 7 Author contribution

LKS planned the sampling and conceptualized the study together with the supervisors TF and AB. TB and JS mentored and reviewed. LKS conducted the statistical analyses with support and supervision by TF and AB. LKS conducted the GIS analysis. ER developed the code and performed the calculations for the snow cover analysis. LKS prepared the original draft including all figures and all authors contributed to the writing of this manuscript.

590

8 Competing interests

The authors declare that they have no conflict of interest.

9 Acknowledgments

595 This work was funded by the DFG Research Training Group "Natural Hazards and Risks in a Changing World" (NatRisk Change GRK 2043/1 and GRK 2043/2) as well as a field work fellowship of the German Hydrological Society (DHG).

We thank the Hydrographic Service of Tyrol, Austria, the TiWAG Tirolean hydropower corporation and the Bavarian Academy of Sciences and Humanities for the provision of data as well as logistical support and fruitful
600 discussions.

We thank Peter Grosse and Marvin Teschner for their support in field, laboratory work and data analyses, Nina Lena Neumann and Joseph Pscherer for their laboratory work and Daniel Bazant for his support during the GIS analysis.

We thank Stefan Achleitner, Carolina Kinzel and the Environmental Engineering laboratory at the University of
605 Innsbruck for their kind support during field and laboratory work.

References

Abermann, J., Lambrecht, A., Fischer, A., and Kuhn, M.: Quantifying changes and trends in glacier area and volume in the Austrian Ötztal Alps (1969-1997-2006), The Cryosphere, 3, 205–215, doi: 10.5194/tc-3-205-2009, 2009.

610 Ballantyne, C. K.: Paraglacial geomorphology, Quat. Sci. Rev., 21, 1935–2017, doi: 10.1016/S0277-3791(02)00005-7, 2002.

Beniston, M., Farinotti, D., Stoffel, M., Andreassen, L. M., Coppola, E., Eckert, N., Fantini, A., Giacona, F., Hauck, C., Huss, M., Huwald, H., Lehning, M., López-Moreno, J.-I., Magnusson, J., Marty, C., Morán-Tejéda, E., Morin, S., Naaim, M., Provenzale, A., Rabatel, A., Six, D., Stötter, J., Strasser, U., Terzago, S., and Vincent,
615 C.: The European mountain cryosphere: a review of its current state, trends, and future challenges, The Cryosphere, 12, 759–794, doi: 10.5194/tc-12-759-2018, 2018.

Beylich, A. A., Laute, K., and Storms, J. E. A.: Contemporary suspended sediment dynamics within two partly glacierized mountain drainage basins in western Norway (Erdalen and Bødalen, inner Nordfjord), Geomorphology, 287, 126–143, doi: 10.1016/j.geomorph.2015.12.013, 2017.

620 Boeckli, L., Brenning, A., Gruber, S., and Noetzli, J.: Permafrost distribution in the European Alps: calculation and evaluation of an index map and summary statistics, The Cryosphere, 6, 807–820, doi: 10.5194/tc-6-807-2012, 2012.

Braun, L. N., Escher-Vetter, H., Siebers, M., and Weber, M.: Water Balance of the highly Glaciated Vernagt Basin, Ötztal Alps, in: The water balance of the alps: what do we need to protect the water resources of the
625 Alps? ; proceedings of the conference held at Innsbruck university, 28 - 29 september 2006, Univ. Press, Innsbruck, 2007.

Buckel, J. and Otto, J.-C.: The Austrian Glacier Inventory GI 4 (2015) in ArcGis (shapefile) format, doi: 10.1594/PANGAEA.887415, 2018.

630 Bürger, G., Pfister, A., and Bronstert, A.: Temperature-Driven Rise in Extreme Sub-Hourly Rainfall, J. Clim., 32, 7597–7609, doi: 10.1175/JCLI-D-19-0136.1, 2019.

Carrivick, J. L. and Heckmann, T.: Short-term geomorphological evolution of proglacial systems, Geomorphology, 287, 3–28, doi: 10.1016/j.geomorph.2017.01.037, 2017.

Cavalli, M., Trevisani, S., Comiti, F., and Marchi, L.: Geomorphometric assessment of spatial sediment connectivity in small Alpine catchments, Geomorphology, 188, 31–41, doi: 10.1016/j.geomorph.2012.05.007, 635 2013.

Chiarle, M., Geertsema, M., Mortara, G., and Clague, J. J.: Relations between climate change and mass movement: Perspectives from the Canadian Cordillera and the European Alps, Glob. Planet. Change, 202, 103499, doi: 10.1016/j.gloplacha.2021.103499, 2021.

Collins, D. N.: Seasonal and annual variations of suspended sediment transport in meltwaters draining from an 640 Alpine glacier, in: Hydrological Measurements; the Water Cycle (Proceedings of two Lausanne Symposia), 9, 1990.

Collins, D. N.: A conceptually based model of the interaction between flowing meltwater and subglacial sediment, Ann. Glaciol., 22, 224–232, doi: 10.3189/1996AoG22-1-224-232, 1996.

Costa, A., Anghileri, D., and Molnar, P.: Hydroclimatic control on suspended sediment dynamics of a regulated 645 Alpine catchment: a conceptual approach, Hydrol. Earth Syst. Sci., 22, 3421–3434, doi: https://doi.org/10.5194/hess-22-3421-2018, 2018.

Delaney, I. and Adhikari, S.: Increased Subglacial Sediment Discharge in a Warming Climate: Consideration of Ice Dynamics, Glacial Erosion, and Fluvial Sediment Transport, Geophys. Res. Lett., 47, e2019GL085672, doi: https://doi.org/10.1029/2019GL085672, 2020.

650 Delaney, I., Bauder, A., Huss, M., and Weidmann, Y.: Proglacial erosion rates and processes in a glacierized catchment in the Swiss Alps, Earth Surf. Process. Landf., 43, 765–778, doi: 10.1002/esp.4239, 2018a.

Delaney, I., Bauder, A., Werder, M., and Farinotti, D.: Regional and annual variability in subglacial sediment transport by water for two glaciers in the Swiss Alps, Front. Earth Sci., 6, 175, doi: 10.3929/ethz-b-000305762, 2018b.

655 Felix, D., Albayrak, I., and Boes, R. M.: In-situ investigation on real-time suspended sediment measurement techniques: Turbidimetry, acoustic attenuation, laser diffraction (LISST) and vibrating tube densimetry, Int. J. Sediment Res., 33, 3–17, doi: 10.1016/j.ijsrc.2017.11.003, 2018.

Fischer, A., Seiser, B., Stocker-Waldhuber, M., and Abermann, J.: The Austrian Glacier Inventory GI 3, 2006, in ArcGIS (shapefile) format, doi: 10.1594/PANGAEA.844985, 2015.

660 Gattermayr, W.: Das hydrographische Regime der Ötztaler Ache, in: E.-M. Koch & B. Erschbamer (Hrsg.), Wetter und Klima im Wandel, vol. 3 Klima, Wetter, Gletscher im Wandel, Innsbruck University Press., Innsbruck, 35, 2013.

Giorgi, F., Torma, C., Coppola, E., Ban, N., Schär, C., and Somot, S.: Enhanced summer convective rainfall at Alpine high elevations in response to climate warming, Nat. Geosci., 9, 584–589, doi: 10.1038/ngeo2761, 2016.

665 Gobiet, A., Kotlarski, S., Beniston, M., Heinrich, G., Rajczak, J., and Stoffel, M.: 21st century climate change in the European Alps—A review, Sci. Total Environ., 493, 1138–1151, doi: 10.1016/j.scitotenv.2013.07.050, 2014.

Guillon, H., Mugnier, J.-L., and Buoncristiani, J.-F.: Proglacial sediment dynamics from daily to seasonal scales in a glaciated Alpine catchment (Bossons glacier, Mont Blanc massif, France), Earth Surf. Process. Landf., 43, 1478–1495, doi: 10.1002/esp.4333, 2018.

670 Hallet, B., Hunter, L., and Bogen, J.: Rates of erosion and sediment evacuation by glaciers: A review of field data and their implications, Glob. Planet. Change, 12, 213–235, doi: 10.1016/0921-8181(95)00021-6, 1996.

Hanus, S., Hrachowitz, M., Zekollari, H., Schoups, G., Vizcaino, M., and Kaitna, R.: Timing and magnitude of future annual runoff extremes in contrasting Alpine catchments in Austria, Hydrol. Earth Syst. Sci. Discuss., 1–35, doi: 10.5194/hess-2021-92, 2021.

675 Hanzer, F., Förster, K., Nemec, J., and Strasser, U.: Projected cryospheric and hydrological impacts of 21st century climate change in the Ötztal Alps (Austria) simulated using a physically based approach, Hydrol. Earth Syst. Sci., 22, 1593–1614, doi: https://doi.org/10.5194/hess-22-1593-2018, 2018.

Hinderer, M., Kastowski, M., Kamelger, A., Bartolini, C., and Schlunegger, F.: River loads and modern denudation of the Alps — A review, Earth-Sci. Rev., 118, 11–44, doi: 10.1016/j.earscirev.2013.01.001, 2013.

680 Hock, R.: 4.5 Hydrologische Veränderungen in vergletscherten Einzugsgebieten, in: Warnsignal Klima: Hochgebirge im Wandel., edited by: Lozán, J. L., Breckle, S.-W., and Graßl, H., 5, 2020.

Hock, R., Jansson, P., and Braun, L. N.: Modelling the Response of Mountain Glacier Discharge to Climate Warming, in: Global Change and Mountain Regions: An Overview of Current Knowledge, edited by: Huber, U. M., Bugmann, H. K. M., and Reasoner, M. A., Springer Netherlands, Dordrecht, 243–252, doi: 10.1007/1-4020-
685 3508-X_25, 2005.

Huggel, C., Salzmann, N., Allen, S., Caplan-Auerbach, J., Fischer, L., Haeberli, W., Larsen, C., Schneider, D., and Wessels, R.: Recent and future warm extreme events and high-mountain slope stability, Philos. Trans. R. Soc. Math. Phys. Eng. Sci., 368, 2435–2459, doi: 10.1098/rsta.2010.0078, 2010.

Huss, M., Bookhagen, B., Huggel, C., Jacobsen, D., Bradley, R. S., Clague, J. J., Vuille, M., Buytaert, W.,
690 Cayan, D. R., Greenwood, G., Mark, B. G., Milner, A. M., Weingartner, R., and Winder, M.: Toward mountains without permanent snow and ice, Earths Future, 5, 418–435, doi: 10.1002/2016EF000514, 2017.

Hydrographic yearbook of Austria, Hydrographisches Jahrbuch von Österreich, Hydrographischer Dienst in Österreich, Bundesministerium für Land- und Forstwirtschaft, Umwelt und Wasserwirtschaft Abteilung VII/3, 2016.

695 Klug, C., Rieg, L., Ott, P., Mössinger, M., Sailer, R., and Stötter, J.: A Multi-Methodological Approach to Determine Permafrost Occurrence and Ground Surface Subsidence in Mountain Terrain, Tyrol, Austria, Permafr. Periglac. Process., 28, 249–265, doi: 10.1002/ppp.1896, 2017.

Kormann, C., Bronstert, A., Francke, T., Recknagel, T., and Graeff, T.: Model-Based Attribution of High-Resolution Streamflow Trends in Two Alpine Basins of Western Austria, Hydrology, 3, 7, doi:
700 10.3390/hydrology3010007, 2016.

Kuhn, M., Nickus, U., and Pellet, F.: Precipitation Patterns in the Inner Ötztal, 17. Internationale Tagung für Alpine Meteorologie, 1982.

Kuhn, M., Helfricht, K., Ortner, M., Landmann, J., and Gurgiser, W.: Liquid water storage in snow and ice in 86 Eastern Alpine basins and its changes from 1970–97 to 1998–2006, Ann. Glaciol., 57, 11–18, doi:
705 10.1017/aog.2016.24, 2016.

Lalk, P., Haimann, M., and Habersack, H.: Monitoring, Analyse und Interpretation des Schwebstofftransportes an österreichischen Flüssen, Österr. Wasser- Abfallwirtsch., 66, 306–315, doi: 10.1007/s00506-014-0175-x, 2014.

Land Tirol: Digital terrain model of Tyrol, 10m resolution, EPSG 31254 [data set],
710 https://www.data.gv.at/katalog/dataset/land-tirol_tirolgelnde, 2016.

Lane, S. N., Bakker, M., Gabbud, C., Micheletti, N., and Saugy, J.-N.: Sediment export, transient landscape response and catchment-scale connectivity following rapid climate warming and Alpine glacier recession, Geomorphology, 277, 210–227, doi: 10.1016/j.geomorph.2016.02.015, 2017.

715 Leggat, M. S., Owens, P. N., Stott, T. A., Forrester, B. J., Déry, S. J., and Menounos, B.: Hydro-meteorological drivers and sources of suspended sediment flux in the pro-glacial zone of the retreating Castle Creek Glacier, Cariboo Mountains, British Columbia, Canada, Earth Surf. Process. Landf., 40, 1542–1559, doi: 10.1002/esp.3755, 2015.

Li, D., Overeem, I., Kettner, A., Zhou, Y., and Xixi, L.: Air Temperature Regulates Erodible Landscape, Water, and Sediment Fluxes in the Permafrost-Dominated Catchment on the Tibetan Plateau, Water Resour. Res., 57,
720 doi: 10.1029/2020WR028193, 2021.

Matiu, M., Jacob, A., and Notarnicola, C.: Daily MODIS Snow Cover Maps for the European Alps from 2002 onwards at 250 m Horizontal Resolution Along with a Nearly Cloud-Free Version, Data, 5, 1, doi: 10.3390/data5010001, 2020.

Merten, G., Capel, P., and Minella, J. P. G.: Effects of suspended sediment concentration and grain size on three
725 optical turbidity sensors, J. Soils Sediments, 14, doi: 10.1007/s11368-013-0813-0, 2014.

Micheletti, N. and Lane, S. N.: Water yield and sediment export in small, partially glaciated Alpine watersheds in a warming climate, Water Resour. Res., 52, 4924–4943, doi: 10.1002/2016WR018774, 2016.

Milliman, J. D. and Syvitski, J. P. M.: Geomorphic/Tectonic Control of Sediment Discharge to the Ocean: The Importance of Small Mountainous Rivers, J. Geol., 100, 525–544, doi: 10.1086/629606, 1992.

730 Orwin, J. F. and Smart, C. C.: Short-term spatial and temporal patterns of suspended sediment transfer in proglacial channels, small River Glacier, Canada, Hydrol. Process., 18, 1521–1542, doi: 10.1002/hyp.1402, 2004.

R Core Team: R: A language and environment for statistical computing., R Foundation for Statistical Computing, Vienna, Austria., 2018.

735 Rottler, E., Francke, T., Bürger, G., and Bronstert, A.: Long-term changes in central European river discharge for 1869–2016: impact of changing snow covers, reservoir constructions and an intensified hydrological cycle, Hydrol. Earth Syst. Sci., 24, 1721–1740, doi: 10.5194/hess-24-1721-2020, 2020.

Rottler, E., Vormoor, K., Francke, T., Warscher, M., Strasser, U., and Bronstert, A.: Elevation-dependent compensation effects in snowmelt in the Rhine River Basin upstream gauge Basel, Hydrol. Res., 52, 536–557,
740 doi: 10.2166/nh.2021.092, 2021.

Savi, S., Comiti, F., and Strecker, M. R.: Pronounced increase in slope instability linked to global warming: A case study from the eastern European Alps, Earth Surf. Process. Landf., 46, doi: https://doi.org/10.1002/esp.5100, 2020.

Scherrer, S. C., Fischer, E. M., Posselt, R., Liniger, M. A., Croci-Maspoli, M., and Knutti, R.: Emerging trends
745 in heavy precipitation and hot temperature extremes in Switzerland, J. Geophys. Res. Atmospheres, 121, 2626–2637, doi: https://doi.org/10.1002/2015JD024634, 2016.

Schmieder, J., Marke, T., and Strasser, U.: Wo kommt das Wasser her? Tracerbasierte Analysen im Rofental (Ötztaler Alpen, Österreich), Österr. Wasser- Abfallwirtsch., 70, 507–514, doi: 10.1007/s00506-018-0502-8, 2018.

750 Schöber, J. and Hofer, B.: The sediment budget of the glacial streams in the catchment area of the Gepatsch reservoir in the Ötztal Alps in the period 1965-2015, ICOLD 2018 Wien Int. Com. Large Dam Syst. Proc., 2018.

Schöber, J., Schneider, K., Helfricht, K., Schattan, P., Achleitner, S., Schöberl, F., and Kirnbauer, R.: Snow cover characteristics in a glacierized catchment in the Tyrolean Alps - Improved spatially distributed modelling by usage of Lidar data, J. Hydrol., 519, 3492–3510, doi: 10.1016/j.jhydrol.2013.12.054, 2014.

755 Sommer, C., Malz, P., Seehaus, T. C., Lippl, S., Zemp, M., and Braun, M. H.: Rapid glacier retreat and downwasting throughout the European Alps in the early 21 st century, Nat. Commun., 11, 3209, doi: 10.1038/s41467-020-16818-0, 2020.

Stoll, E., Hanzer, F., Oesterle, F., Nemec, J., Schöber, J., Huttenlau, M., and Förster, K.: What Can We Learn from Comparing Glacio-Hydrological Models?, Atmosphere, 11, 981, doi: 10.3390/atmos11090981, 2020.

760 Strasser, U., Marke, T., Braun, L., Escher-Vetter, H., Juen, I., Kuhn, M., Maussion, F., Mayer, C., Nicholson, L., Niedertscheider, K., Sailer, R., Stötter, J., Weber, M., and Kaser, G.: The Rofental: a high Alpine research basin (1890–3770 m a.s.l.) in the Ötztal Alps (Austria) with over 150 years of hydrometeorological and glaciological observations, Earth Syst. Sci. Data, 10, 151–171, doi: https://doi.org/10.5194/essd-10-151-2018, 2018.

Swift, D. A., Nienow, P. W., and Hoey, T. B.: Basal sediment evacuation by subglacial meltwater: suspended
765 sediment transport from Haut Glacier d'Arolla, Switzerland, Earth Surf. Process. Landf., 30, 867–883, doi: 10.1002/esp.1197, 2005.

Tiel, M. van, Kohn, I., Loon, A. F. V., and Stahl, K.: The compensating effect of glaciers: Characterizing the relation between interannual streamflow variability and glacier cover, Hydrol. Process., 34, doi: 10.1002/hyp.13603, 2019.

770 Tschada, H. and Hofer, B.: Total solids load from the catchment area of the Kaunertal hydroelectric power station: the results of 25 years of operation, in: Hydrology in Mountain Regions. II - Artificial Reservoirs; Waters and Slopes (Proceedings of two Lausanne Symposia), 8, 1990.

Tsyplenkov, A., Vanmaercke, M., Golosov, V., and Chalov, S.: Suspended sediment budget and intra-event sediment dynamics of a small glaciated mountainous catchment in the Northern Caucasus, J. Soils Sediments,
775 20, 3266–3281, doi: 10.1007/s11368-020-02633-z, 2020.

Umweltbundesamt: CORINE Landcover 2018 [data set], https://www.data.gv.at/katalog/dataset/clc2018, 2018.

Vercruysse, K., Grabowski, R. C., and Rickson, R. J.: Suspended sediment transport dynamics in rivers: Multi-scale drivers of temporal variation, Earth-Sci. Rev., 166, 38–52, doi: 10.1016/j.earscirev.2016.12.016, 2017.

Vormoor, K., Lawrence, D., Heistermann, M., and Bronstert, A.: Climate change impacts on the seasonality and
780 generation processes of floods – projections and uncertainties for catchments with mixed snowmelt/rainfall regimes, Hydrol. Earth Syst. Sci., 19, 913–931, doi: 10.5194/hess-19-913-2015, 2015.

Weber, M. and Prasch, M.: Influence of the Glaciers on Runoff Regime and Its Change, Reg. Assess. Glob. Change Impacts, 493–509, doi: 10.1007/978-3-319-16751-0_56, 2016.

Wijngaard, R. R., Helfricht, K., Schneeberger, K., Huttenlau, M., Schneider, K., and Bierkens, M. F. P.:
785 Hydrological response of the Ötztal glacierized catchments to climate change, Hydrol. Res., 47, 979–995, doi: 10.2166/nh.2015.093, 2016.

World Glacier Monitoring Service: Fluctuations of Glaciers Database, WGMS [data set], doi: 10.5904/wgms-fog-2021-05, 2021.

Wulf, H., Bookhagen, B., and Scherler, D.: Climatic and geologic controls on suspended sediment flux in the
790 Sutlej River Valley, western Himalaya, Hydrol. Earth Syst. Sci., 16, 2193–2217, doi: 10.5194/hess-16-2193-2012, 2012.

Zentralanstalt für Meteorologie und Geodynamik (ZAMG), Climate Data of Austria 1971 - 2000: www.zamg.ac.at/fix/klima/oe71-00/klima2000/klimadaten_oesterreich_1971_frame1.htm, 2013.